# Locating Fiber Loss Anomalies with a Receiver-side Monitoring Algorithm exploiting Cross-Phase Modulation

**P. Serena[1*], C. Lasagni[2], A. Bononi[1], F. Boitier[3], A. May[3], P. Ramantanis[3] and M. Lonardi[3]**

[1] *Department of Engineering and Architecture, University of Parma, 43124, Parma, Italy*
[2] *Department of Physical and Chemical Sciences, University of l'Aquila, 67100, l'Aquila, Italy*
[3] *Nokia Bell Labs, Route de Villejust, 91620, Nozay, France*

[*] *paolo.serena@unipr.it*

**Abstract:** We propose and experimentally test a cross-phase modulation based algorithm to monitor network loss anomalies from detected data. The idea does not need service interruption, special signals, nor an exhaustive search of the anomaly coordinate. 

## 1. Introduction

Monitoring the physical parameters of an optical link is of great importance to estimate soft network failures and to reduce extra operational margins set during the network design [1,2]. The task can be accomplished by monitoring optical signals at intermediate nodes of the network, or by processing the electrical signal under detection at a given coherent receiver. The latter is of particular relevance since it provides parameter estimation in a plug-and-play fashion, reducing costs and simplifying the network monitoring. In the literature, edge-side monitoring techniques have been developed by exploiting the non-commutative interaction between Kerr and dispersive fiber effects through the capabilities offered by coherent detection. Of particular relevance are the fiber-longitudinal monitor methods based on back-propagation techniques [3,4] that provide a tomography of the optical link by scanning the coordinates one by one. The corresponding algorithms have been further optimized [5,6] and extended to estimate more complex network scenarios [7] or spectral gain profiles of amplifiers [8].

However, such techniques suffer from some limitations. For instance, high powers of the channel under test (CUT) are desirable to emphasize nonlinearity through self-phase modulation (SPM). Moreover, such techniques may suffer from ambiguities and require many discrete Fourier transforms. A technique based on cross-phase modulation (XPM) was proposed in [9], but it requires special sequences and operation during maintenance mode.

In this work, we exploit XPM between an auxiliary channel (e.g., through a super-channel) and the CUT to detect the coordinate of loss anomalies with a resolution of a few km. The proposed method does not require special power allocations or Tx/Rx, nor an exhaustive anomaly search. It exploits the localized nature of nonlinear pulse collisions during propagation [10].

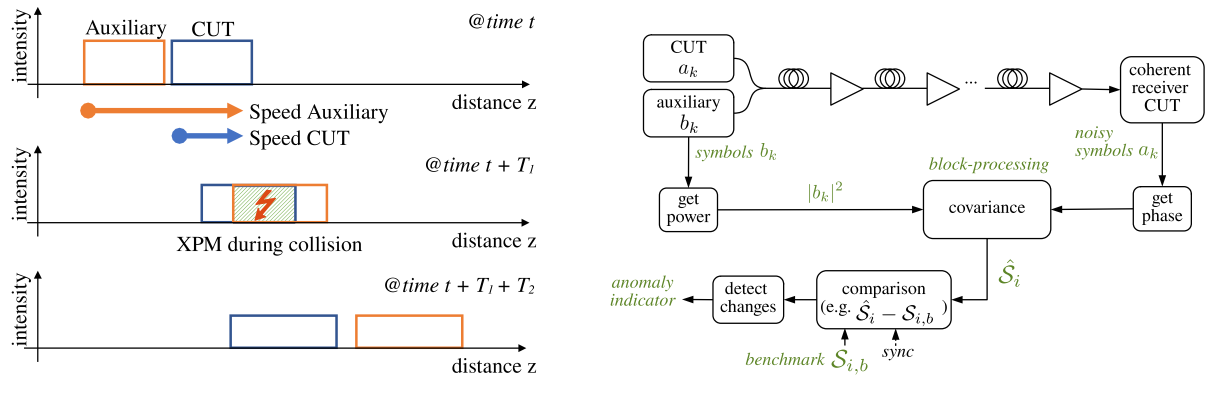


Fig. 1. Left: example of two-pulse collision. Right: the proposed algorithm for anomaly detection.

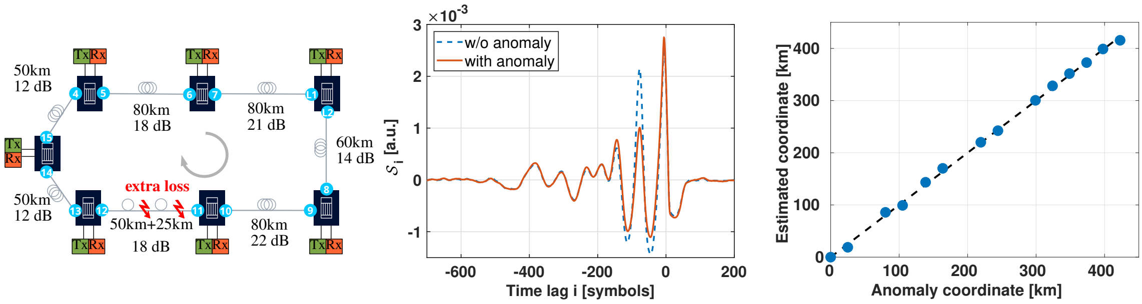


Fig. 2. Experimental results. Left: setup. An extra loss (3 dB) is placed in correspondence with one red arrow. The Tx/Rx signals are injected/detected at a given ROADM. Center: phase impulse response given by the algorithm of Fig. 1 without anomaly (dashed) and with anomaly after 80 km (solid). Right: estimated anomaly coordinate.

## 2. Pulse-collision based monitoring

Two channels propagating in an optical fiber interact through XPM. In the time domain, XPM is the result of collisions among pump channel pulses with probe channel (aka CUT) pulses. In general, four pulses collide, three coming from the nonlinear Kerr effect, and one from the matched filter impulse response [10]. Such collisions are localized in specific link sections since the pulses travel at different speeds. Therefore, the interaction contains a signature of the local link's physical properties during the collision. To extract such information, we focus on two-pulse collisions, which, under perturbative assumptions, induce only a phase distortion $\varphi_i = -\sum_k |b_k|^2 \mathcal{S}_{i-k}$ on the detected $i$th CUT symbol [10], where $b_k$ are the known complex symbols of the interfering channel. The discrete-time impulse response $\mathcal{S}_i$ weighting such collisions along time $t$ and distance $z$ is:

$$\mathcal{S}_i = \frac{8}{9}\gamma \int_0^{L_t} f(z) \int_{-\infty}^{\infty} |p(z, t + iT - \tau(z))|^2 |p(z,t)|^2 \mathrm{d}t\mathrm{d}z \tag{1}$$

with $\gamma$ the fiber nonlinear coefficient, $f(z)$ the link power profile, $L_t$ the link length, $T$ symbol time. $\tau(z)$ is the channel walk-off that plays a fundamental role in localizing the collision, see Fig. 1 (left) for a sketch. $p(z,t)$ is the pulse distorted by chromatic dispersion only. For instance, in typical fibers, and with sinc transmitted pulses, after a few tens of km $|p(z,t)|^2$ takes a rectangular shape in intensity [10], of width linearly increasing with $z$. Although (1) has been introduced in scalar propagation, its generalization to dual polarization is straightforward [10].

To localize the anomaly we monitor $\mathcal{S}_i$. Since $\mathcal{S}_i$ relates $\varphi_i$ and $|b_i|^2$ through a convolution, its minimum mean-square error estimate is, according to Wiener filter theory, proportional to the covariance between $\varphi_i$ and $|b_i|^2$, which can be efficiently estimated by averaging the convolution $\left(|b_i|^2 - \mathbb{E}[|b_i|^2]\right) \otimes (\varphi_i - \mathbb{E}[\varphi_i])$, with $\mathbb{E}$ expectation. The key point is that the time lags $i$ are uniquely related to the starting/ending coordinate of the collision through the channel walk-off, hence i) each $i$ sample of $\mathcal{S}_i$ contains a localized signature of the link, ii) by a convolution we explore all coordinates at once. Some impairments affecting the estimation, such as amplified spontaneous emission (ASE), SPM, three-, and four-pulse collisions, are averaged to zero by collecting samples. We are thus demanding time for averaging rather than complexity in the chip area. Nevertheless, with data rates of the order of Gbd, the anomaly can be localized in seconds. Finally, by comparing $\mathcal{S}_i$ with a benchmark one an anomaly can be detected. The block diagram of the proposed algorithm is given in Fig. 1 (right).

## 3. Experimental and numerical investigations

We experimentally investigated the proposed anomaly detector by the testbed depicted in Fig. 2 (left). It describes a 470 km demo ring network composed of seven nodes. Each node contained two optical amplifiers and a reconfigurable optical add-drop multiplexer (ROADM). The network was loaded with ASE channels. The CUT was a 33.6 Gbd polarization-division multiplexed quadrature amplitude modulation (PDM-4QAM) channel generated by a commercial Nokia transponder (1830 PSI-2T) in alphabet four. The auxiliary channel was a 32 Gbd PDM-16QAM signal driven by a $2^{16}$ pseudo-random sequence with a spacing of $\Delta f_{cs} = 200$ GHz to the CUT. We collected 670 Msymbols to better average out any non-two-pulse collision. Each channel had a power of 5 dBm and a pulse roll-off $\rho = 0.4$ (in numerical simulations we observed essentially no impact of $\rho$). The average fiber dispersion was 16.8 ps/nm/km, while the average fiber attenuation coefficient was 0.24 dB/km. We launched the CUT and the auxiliary channel at the same node and detected the CUT after a round-trip. The anomaly was a 3 dB optical attenuator placed at the beginning or after 25 km of a given span, see the red arrows in Fig. 2 (left). We tested

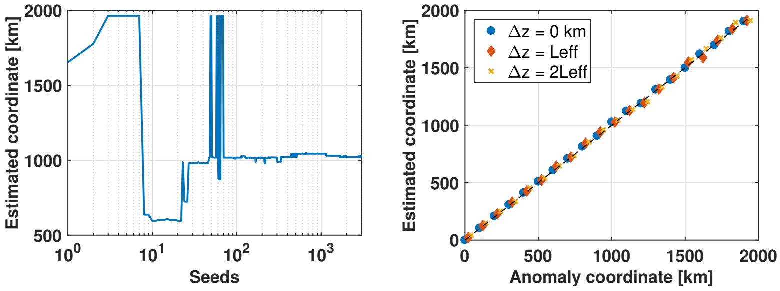


Fig. 3. Numerical results. Left: convergence rate vs number of random seeds with 3 dB loss anomaly at 1000 km (65536 symbols/seed). 9 × 75 GHz 16QAM. Right: estimated coordinate with anomaly placed $\Delta z$ km from the beginning of a span, with $\Delta f_{cs} = 300$ GHz, only XPM. 20 × 100 km link.

injecting the signals sequentially in all ROADM, which is equivalent to varying the anomaly coordinate along the link. We detected the CUT by a coherent receiver and a 200 Gsample/s real-time oscilloscope.

Figure 2 (center) shows an example of $\mathcal{S}_i$, smoothed over 50 taps, estimated with/without an anomaly at 80 km. $\mathcal{S}_i$ shows an oscillating profile, with local minima approximately indicating the start of a new span. The effect of the anomaly is visible by comparison. Different techniques are possible to convert such information into an anomaly location. We estimated the anomaly coordinate by i) finding the time lag of maximum $\mathcal{S}_i$ difference, ii) converting it into a coordinate of maximum collision (pulse overlap) by exploiting the time-to-distance mapping through the walk-off, and iii) removing the estimation bias of the coordinate of the anomaly after 0 km. The results are depicted in Fig. 2 (right). The match is very good, with a root mean square error (RMSE) of 4.3 km.

We tested the algorithm for longer links through numerical simulations. Here we sent two 0 dBm, 64 Gbd, 16QAM channels, $\Delta f_{cs} = 300$ GHz, in a $20 \times 100$ km link. The 3 dB loss anomaly was placed at the beginning ($\Delta z = 0$ km), after one, or two effective lengths ($L_{eff} = 21.5$ km) of a span. We used 65536 random symbols for each run, i.e., seed. We first run fast tests without ASE and SPM, obtaining good results, see Fig. 3 (right). The most accurate estimations are for anomalies placed at $\Delta z = 0$ km, where the Kerr effect is maximum. Overall, the RMSE after 98 Msymbols is 16 km. To check the impact of ASE,SPM, and extra XPM on the estimation accuracy, in Fig. 3 (left) we show the estimated coordinate with the anomaly at 1000 km in the presence of 9 channels (spacing 75 GHz) and in-line ASE (noise figure 6 dB). Smaller RMSE can be achieved for increasing seeds, i.e., longer averaging.

## 4. Conclusions

We proposed an XPM-based monitoring technique and experimentally/numerically tested it to locate loss anomalies. The method needs an auxiliary channel traveling with the CUT. It does not need special power allocations or sequences, and monitors all link coordinates at once, without the need for an exhaustive search.

This work was supported by the Italian government through the project PRIN 2017 (FIRST) and the EU H2020 within B5G-OPEN, grant agreement 101016663.

## References

1. Y. Pointurier, "Design of low-margin optical networks," *J. Opt. Commun. Netw.*, vol. 9, no. 1, pp. A9–A17, 2017.
2. T. Tanimura, S. Yoshida, K. Tajima, S. Oda, and T. Hoshida, "Concept and implementation study of advanced DSP-based fiber-longitudinal optical power profile monitoring toward optical network tomography," *J. Opt. Commun. Netw.*, vol. 13, no. 10, pp. E132–E141, 2021.
3. T. Tanimura, S. Yoshida, K. Tajima, S. Oda, and T. Hoshida, "Fiber-Longitudinal Anomaly Position Identification over Multi-Span Transmission Link out of Receiver-end Signals," *J. Lightw. Technol.*, vol. 38, no. 9, pp. 2726–2733, 2020.
4. T. Sasai, M. Nakamura, E. Yamazaki, S. Yamamoto, H. Nishizawa, and Y. Kisaka, "Digital Longitudinal Monitoring of Optical Fiber Communication Link," *J. Lightw. Technol.*, vol. 40, no. 8, pp. 2390–2408, 2021.
5. T. Sasai, M. Nakamura, E. Yamazaki, and Y. Kisaka, "Precise Longitudinal Power Monitoring over 2080 km Enabled by Step Size Selection of Split Step Fourier Method," in Proc. *Opt. Fiber Commun. Conf. Expo.*, San Diego, CA, USA, Art. no. Th1C.4, 2020.
6. T. Sasai, E. Yamazaki, M. Nakamura, and Y. Kisaka, "Proposal of Linear Least Squares for Fiber- Nonlinearity-Based Longitudinal Power Monitoring in Multi-Span Link," in Proc. *OECC/PSC*, Toyama, Japan, Art. no. WB3-1, 2022.
7. A. May, F. Boitier, A. Courilleau, B. A. Ayoubi, and P. Layec, "Demonstration of Enhanced Power Losses Characterization in Optical Networks," in Proc. *Opt. Fiber Commun. Conf. Expo.*, San Diego, CA, USA, Art. no. Th1C.6, 2022.
8. M. Sena et al., "DSP-Based Link Tomography for Amplifier Gain Estimation and Anomaly Detection in C+L-Band Systems," *J. Lightw. Technol.*, vol. 40, no. 11, pp. 3395–3405, 2022.
9. R. Hui, C. Laperle, and M. O'Sullivan, "Measurement of Total and Longitudinal Nonlinear Phase Shift as Well as Longitudinal Dispersion for a Fiber-Optic Link Using a Digital Coherent Transceiver," *J. Lightw. Technol.*, (early access), 2022.
10. R. Dar, M. Feder, A. Mecozzi, and M. Shtaif, "Pulse collision picture of inter-channel nonlinear interference noise in fiber-optic communications," *J. Lightw. Technol.*, vol. 34, no. 2, pp. 593–607, 2016.